INTERNATIONAL JOURNAL FOR NUMERICAL METHODS IN FLUIDS, VOL. 8, 227–242 (1988)

THE BOUNDARY INTEGRAL EQUATION METHOD FOR THE SOLUTION OF WAVE–OBSTACLE INTERACTION

K. J. WILLIAMS

Department of Civil Engineering, University of Glasgow, Glasgow, U.K.

SUMMARY

The boundary integral equation method constitutes the basis of a number of computer programs used for the solution of wave–obstacle interaction problems. For the case of obstacles in a constant depth fluid, the method assumes that the velocity potential at any point in the fluid may be represented by a distribution of Green's function sources over the immersed surface of the obstacle. Application of the obstacle kinematic boundary condition gives rise to an integral equation which may be solved, using numerical discretization, for the unknown source strength distribution function. Subsequent evaluation of the discretized velocity potential permits evaluation of the hydrodynamic interaction parameters.

A series of numerical solutions have been carried out for a range of substantially rectangular obstacles, in a two-dimensional domain, using varying levels of immersed profile discretization. The results, presented in the form of fixed and floating mode wave reflection and transmission, together with the motion response of the floating obstacle, demonstrate the significant sensitivity of the evaluated parameters to variations in the level of discretization.

KEY WORDS Wave–source distribution Green's function discretization

INTRODUCTION

A number of mechanisms give rise to the hydrodynamic forces and wave effects associated with the interaction between a fixed structure and a train of incident waves. The governing mechanisms are determined by the geometry and location of the obstacle, together with its size in relation to the incident wave field. If the characteristic dimension of the structure is significant with respect to the incident wavelength, sufficient to result in deformation of the ambient wave field, the waves undergo significant diffraction. The structure is thus subjected to a diffraction force in addition to the inertial force resulting from the mass displacement of fluid. It is assumed in such a regime that the drag force becomes insignificant and may be neglected, permitting the formulation of a potential theory problem. Consideration of the appropriate boundary conditions enables a solution to be obtained for the diffracted wave potential and subsequent evaluation of the hydrodynamic force components. If the structure is floating, additional boundary value problems are required for each degree of motional freedom, the solutions of which permit the evaluation of its components of motion together with the potentials relating to the waves generated by each mode of body motion.

A number of methods have been employed for the formulation and solution of these boundary value problems but, with the exception of a few simple fixed obstacle geometries, no exact solutions are available and the required solutions must be obtained by numerical means.

0271–2091/88/020227–16$08.00

Received 6 January 1987

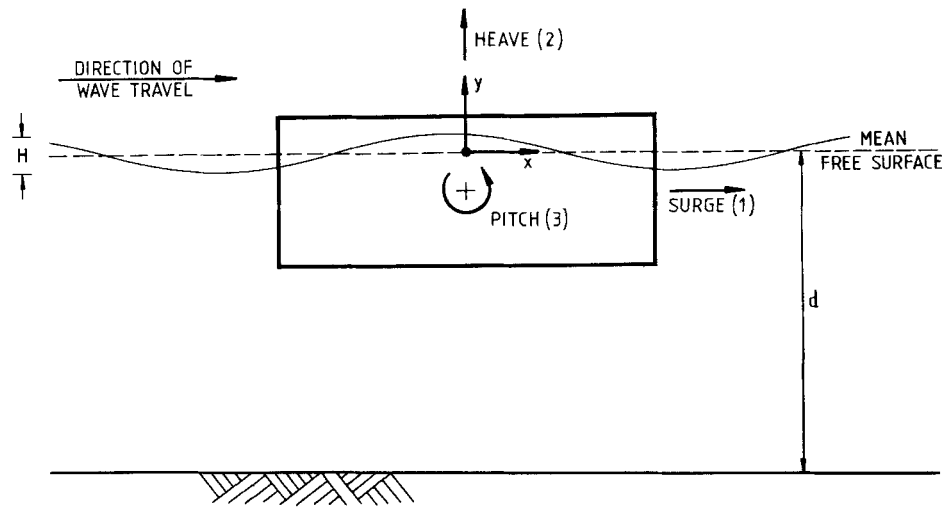

Figure 1. Definitions for floating body analysis

The boundary integral equation method, involving the development of a surface integral equation which may be solved by discretization, has become firmly established in practice and constitutes the basis of a considerable number of computer programs used for the numerical solution of the wave diffraction and radiation problem.

FORMULATION OF THE PROBLEM

Consider the motion of the two-dimensional system consisting of a long floating object partly immersed in an incompressible and inviscid fluid as indicated in Figure 1. The fluid is bounded by a fixed horizontal and impermeable bottom at $y = -d$, the immersed surface of the object denoted by $\Gamma(x, y) = 0$ and the mean free surface of the fluid at $y = 0$ which is assumed to extend longitudinally to infinity in both directions. Assuming the fluid motion to be irrotational, the flow field for an incident train of regular waves may be completely described by a velocity potential, defined in complex form as

$$\Phi(x, y; t) = \mathrm{Re}\,[\phi(x, y)\mathrm{e}^{-\mathrm{i}\sigma t}], \tag{1}$$

where $Re[\ ]$ denotes the real part of the complex expression and σ denotes the incident wave radial frequency ($= 2\pi f$). The time parameter t is understood to be real throughout. The additional assumption is made that the waves are of small amplitude and that the resulting harmonic body motions defined in Figure 1 are also of small amplitude, thus permitting the mathematical problem to be much simplified by linearization.

When the body length is significant with regard to the incident wavelength, the incident waves undergo significant scattering or diffraction. The situation may therefore be conveniently considered in terms of a combination of two fundamental and related problems:

(1) the scattering (or diffraction) problem of an incident wave train interacting with a fixed body;
(2) the wave generation problem of a body forced to oscillate in otherwise still water.

Resulting from the above mathematical linearization, these two motions may be superposed with the wave forces of the scattering problem providing the forcing function in the wave generation

problem, thus permitting expression of the potential as the sum of three separate components:

$$\Phi = \Phi_W + \Phi_S + \Phi_G, \tag{2}$$

where Φ_W is the known potential of the incident waves, Φ_S is the unknown potential of the scattered waves and Φ_G is the unknown potential of the waves generated by body motion. The following conditions are satisfied by each of the three components:

(a) The Laplace equation

$$\nabla^2 \Phi(x, y; t) = 0, \quad \text{where} \quad \nabla \equiv \left[\frac{\partial}{\partial x}, \frac{\partial}{\partial y}\right]^T \tag{3}$$

(b) The bottom boundary condition

$$\frac{\partial \Phi(x, y; t)}{\partial y} = 0 \quad \text{at} \quad y = -d. \tag{4}$$

(c) The linearized free surface boundary condition

$$\frac{\partial^2 \Phi(x, y; t)}{\partial t^2} + g \frac{\partial \Phi(x, y; t)}{\partial y} = 0 \quad \text{at} \quad y = 0. \tag{5}$$

(d) The kinematic boundary condition on the immersed surface of the body

$$\frac{\partial \Phi(x, y; t)}{\partial n} = V_n(x, y; t), \tag{6}$$

where V_n is defined by

$$V_n = \mathrm{Re}[v_n(x, y) e^{-i\sigma t}] \quad \text{on} \quad \Gamma(x, y) = 0,$$

where $v_n(x, y)$ denotes the complex function which represents the spatial normal component of velocity on the immersed surface. Following the superposition postulations made previously, equation (6) may be subdivided into the following equations:

$$\frac{\partial \Phi_W}{\partial n} + \frac{\partial \Phi_S}{\partial n} = 0 \quad \text{on} \quad \Gamma(x, y) = 0, \tag{7a}$$

$$\frac{\partial \Phi_G}{\partial n} = V_n \quad \text{on} \quad \Gamma(x, y) = 0. \tag{7b}$$

(e) The potentials pertaining to the scattered and generated waves must, in addition, satisfy the far-field radiation condition guaranteeing that the waves are outgoing and have proper amplitude behaviour at infinity:

$$\lim_{|x| \to \infty} |x|^{1/2} \left(\frac{\partial \phi}{\partial |x|} - ik\phi(x, y) \right) = 0, \tag{8}$$

where $\phi \equiv \phi_S$ and ϕ_G respectively and k is the incident wave number $(2\pi/L)$ defined by the dispersion equation

$$\sigma^2 = gk \tanh(kd), \tag{9}$$

where L is the incident wavelength.

THE INTEGRAL EQUATION FORMULATION

It may be shown[1] that the velocity potential at any point in the fluid domain may be represented by a distribution of pulsating sources of unknown strength over a source boundary:

$$\Phi(\mathbf{x};t) = \int_S f(\xi)G(\mathbf{x},\xi;t)\,\mathrm{d}S, \tag{10}$$

where $\mathbf{x} = (x, y)$ and represents a point in the fluid domain (field point), $\xi = (a, b)$ and represents a point on the source boundary (source point), $f(\xi)$ represents the unknown source strength distribution function and the integration is performed over the source distribution boundary. In order for the representation in equation (10) to be valid, the Green function (source potential) $G(\mathbf{x}, \xi; t)$ must satisfy all the boundary conditions of the problem, given by equations (3), (4), (5) and (7), with the exception of the kinematic boundary condition on the immersed surface of the body.

Such a function has been constructed by Wehausen and Laitone[2] and is defined, in complex form, for the two-dimensional case as

$$G(x, y; a, b; t) = g(x, y; a, b)\mathrm{e}^{-\mathrm{i}\sigma t}, \tag{11}$$

where

$$g(x, y; a, b) = g_1(x, y; a, b) + \mathrm{i}g_2(x, y; a, b),$$

$$g_2(x, y; a, b) = -g_0(y, b)\cos[k(x-a)],$$

$$g_0(y, b) = \frac{2\pi v}{k}\frac{\cosh[k(d+b)]\cosh[k(d+y)]}{vd + \sinh^2(kd)}$$

and $v = \sigma^2/g$ and represents the deep water ($kd \geqslant 5$) wave number. The real part of the Green function is defined in two alternative forms:

The integral form

$$g_1 = \ln(r/d) + \ln(r^2/d) - 2I_1, \tag{12}$$

where

$$r^2 = (x-a)^2 + (y-b)^2,$$

$$r_2^2 = (x-a)^2 + (y+2d+b)^2$$

$$I_1 = \int_0^\infty \left(\frac{\mu + v}{\mu} \frac{\mathrm{e}^{-\mu d}\cosh[\mu(d+b)]\cosh[\mu(d+y)]\cos[\mu(x-a)]}{\mu\sinh(\mu d) - v\cosh(\mu d)} + \frac{\mathrm{e}^{-\mu d}}{\mu} \right) \mathrm{d}\mu,$$

with $\int$ denoting the Cauchy principal value integral.

The series form

$$g_1(x, y; a, b) = g_0(y, b)\sin(k|x-a|)$$

$$-2\pi \sum_{m=1}^{\infty} \frac{1}{\mu_m} C_m \cos[\mu_m(d+y)]\cos[\mu_m(b+d)]\mathrm{e}^{-\mu_m|x-a|},$$

where $\mu_m (m \geqslant 1)$ are the positive real roots of

$$\mu_m \tan(\mu_m d) + v = 0$$

and

$$C_m = \frac{\mu_m^2 + v^2}{\mu_m^2 d + v^2 d - v}.$$

It is generally accepted[3] that the series form of the Green function is more efficiently evaluated than the integral form except in cases where $|x - a|$ is small.

Since Φ and G are harmonic functions, equation (8) may be written in terms of spatial functions only:

$$\phi(\mathbf{x}) = \int_S f(\xi) g(\mathbf{x}, \xi)\, \mathrm{d}S. \tag{14}$$

If the source distribution boundary is chosen to coincide with the immersed surface of the body, application of the kinematic boundary condition, equation (6), to equation (14) yields the following integral equations in terms of the scattered and generated potentials:

$$\frac{\partial \phi_S}{\partial n}(\mathbf{x}) = \int_\Gamma f_S(\xi) \frac{\partial g(\mathbf{x}, \xi)}{\partial n} \mathrm{d}\Gamma + \pi f_S(\mathbf{x}) \quad \text{(scattered wave)}, \tag{15a}$$

$$\frac{\partial \phi_G}{\partial n}(\mathbf{x}) = \int_\Gamma f_G(\xi) \frac{\partial g(\mathbf{x}, \xi)}{\partial n} \mathrm{d}\Gamma + \pi f_G(\mathbf{x}) \quad \text{(generated wave)}, \tag{15b}$$

where the last terms in the equations arise from consideration of the effect of a source at its own point of action and the integrations are performed over the immersed profile of the body.

NUMERICAL SOLUTION

If the directions of motion are defined as surge ≡ mode 1, heave ≡ mode 2, pitch ≡ mode 3 and, in addition, scattering ≡ mode 4, equations (15) may be expressed using index notation as

$$\pi f_m(\mathbf{x}) + \int_\Gamma f_m(\xi) \frac{\partial g(\mathbf{x}, \xi)}{\partial n} \mathrm{d}\Gamma = \frac{\partial \phi_m(\mathbf{x})}{\partial n}, \quad m = 1, 4. \tag{16}$$

Equation (16) may be solved numerically, beginning with subdivision of the immersed surface of the body into N elements of length $\Delta\Gamma_j (j = 1, 2, \ldots, N)$ and identifying as node points the centroid of each element. The assumption may be made that the source strength distribution function $f(\xi)$ is constant over each element.

Since the regular parts of the Green function and its normal gradient oscillate with a wavelength of magnitude comparable with that of the incident wave, it is valid to assume constant function values over each element length providing the elements are small in comparison with the incident wavelength.

Equation (16) may therefore be expressed in discretized form as

$$\pi f_m(\mathbf{x}_i) + \sum_{j=1}^{N} f_m(\xi_j) \frac{\partial g(\mathbf{x}_i, \xi_j)}{\partial n} \Delta\Gamma_j = \frac{\partial \phi_m(\mathbf{x}_i)}{\partial n}, \quad m = 1, 4. \tag{17}$$

The three modes of oscillation of the body may be defined thus:

$$\alpha_m = a_m \mathrm{e}^{-\mathrm{i}\sigma t}, \quad m = 1, 2, 3, \tag{18}$$

where α_m is a translation for $m = 1$ and 2, a rotation for $m = 3$ and a_m is the corresponding complex amplitude of motion.

It is convenient[4] to decompose the generated wave potential Φ_G into three components associated with each degree of freedom and proportional to the modal displacement amplitudes:

$$\Phi_G = \sum_{m=1}^{3} \alpha_m \phi_m^{(g)}. \tag{19}$$

Similarly, the normal velocity may be decomposed as

$$V_n = \sum_{m=1}^{3} \frac{\partial \alpha_m}{\partial t} n_m, \tag{20}$$

where n_m represents the outward normal component scalar of velocity on the immersed surface of the body.

A little algebra involving equations (18)–(20) yields

$$\frac{\partial \phi_m(\mathbf{x}_i)}{\partial n} = -\mathrm{i}\sigma n_m(\mathbf{x}_i), \quad m = 1, 2, 3. \tag{21a}$$

From equation (7a)

$$\frac{\partial \phi_m(\mathbf{x}_i)}{\partial n} = -\frac{\partial \phi_{\mathrm{W}}(\mathbf{x}_i)}{\partial n}, \quad m = 1, 2, 3, \tag{21b}$$

where ϕ_{W} is the potential of the incident wave, defined in complex form as

$$\Phi_{\mathrm{W}} = -\frac{\mathrm{i}gH}{2\sigma} \frac{\cosh[k(d+y)]}{\cosh(kd)} \mathrm{e}^{\mathrm{i}(kx-\sigma t)}, \tag{22}$$

where H is the incident wave height. Substitution of equations (21) in (17) results in the matrix equation

$$\underset{(N,N)}{[\mathbf{A}]} \quad \underset{(N,m)}{[\mathbf{f}]} = \underset{(N,m)}{[\mathbf{B}]}, \tag{23}$$

where

$$A_{ij} = \pi\delta_{ij} + \Delta\Gamma_j \frac{\partial g(\mathbf{x}_i, \boldsymbol{\xi}_j)}{\partial n},$$

$$B_{im} = -\mathrm{i}\sigma n_m(\mathbf{x}_i) \quad \text{for} \quad m = 1, 2, 3,$$

$$B_{im} = -\frac{\partial \phi_{\mathrm{W}}(\mathbf{x}_i)}{\partial n} \quad \text{for} \quad m = 4$$

and δ_{ij} is the Kronecker delta. Equation (23) may be solved for the unknown source distribution matrix $[\mathbf{f}]$, where $f_{jm} = f_m(\xi_j)$ as defined in equation (17).

The velocity potential may be evaluated using the discretized form of equation (14):

$$\phi_m(\mathbf{x}_i) = \sum_{j=1}^{N} f_m(\boldsymbol{\xi}_j) g(\mathbf{x}_i, \boldsymbol{\xi}_j) \Delta_j, \quad i = 1, 2, \ldots, N. \tag{24}$$

HYDRODYNAMIC INTERACTION PARAMETERS

Using the equations of motion[5] adapted for the two-dimensional case, in conjunction with the previously stated potential and velocity decompositions, yields

$$\mu_{ij} = \frac{\rho}{\sigma} \int_{\Gamma} \mathrm{Im}(\phi_j^{(\mathrm{g})}) n_i \, \mathrm{d}\Gamma, \tag{25a}$$

$$\lambda_{ij} = -\rho \int_{\Gamma} \mathrm{Re}(\phi_j^{(\mathrm{g})}) n_i \, \mathrm{d}\Gamma, \tag{25b}$$

where μ_{ij} and λ_{ij} are the added mass and damping coefficients in the ith direction due to motion in the jth direction.

Using the method detailed by Sarpkaya and Isaacson,[4] in conjunction with the well known Haskind relations,[6] the exciting force components may be computed from

$$F_i = F_{0_i} e^{-i\sigma t}, \tag{26}$$

where

$$F_{0_i} = \rho\left[\int_\Gamma \left(\phi_W \frac{\partial \phi_i^{(g)}}{\partial n} - \phi_i^{(g)} \frac{\partial \phi_W}{\partial n}\right) d\Gamma\right], \quad i = 1, 2, 3,$$

thus demonstrating the usefulness of the Haskind relations in that the evaluation of the exciting force components does not necessitate the prior evaluation of the scattered potential.

The complex amplitudes of body motion may be subsequently evaluated from

$$F_{0_i} = \sum_{j=1}^{3} \{[-\sigma^2(m_{ij} + \mu_{ij}) - i\sigma\lambda_{ij} + c_{ij}]a_j\} \tag{27}$$

where m_{11}, m_{22} represent the mass of the floating body, m_{33} is the rotational moment of inertia of the floating body in the pitch mode, $c_{22} = \rho_w g L_w, c_{33} = \rho_w g \mathcal{V} H_3, \rho_w$ is the mass density of water, L_w is the waterline area per unit width of body, $\mathcal{V}$ is the displaced volume per unit width of body, H_3 is the pitch metacentric height and all other c_{ij}, m_{ij} are zero. If the body is subject to any spring restraints to prevent drifting or to simulate mooring conditions, the spring constants may be added to the c_{ij} terms.

Defining the far-field reflection and transmission coefficients as the ratio of the reflected and transmitted wave amplitudes to the incident wave amplitudes, the coefficients may be evaluated from the asymptotic velocity potential expressions thus:

$$Te^{-i\beta_T} = T^{(s)} e^{-i\beta_T^{(s)}} + \sum_{j=1}^{3} T_j^{(g)} e^{-i\beta_{T_j}^{(g)}} = 1 + \frac{2i\sigma}{gH}\left(I_1^{(s)} + \sum_{j=1}^{3} a_j I_{1_j}^{(g)}\right), \tag{28a}$$

$$Re^{-i\beta_R} = R^{(s)} e^{-i\beta_R^{(s)}} + \sum_{j=1}^{3} R_j^{(g)} e^{-i\beta_{R_j}^{(g)}} = \frac{2i\sigma}{gH}\left(I_2^{(s)} + \sum_{j=1}^{3} a_j I_{2_j}^{(g)}\right), \tag{28b}$$

where

$$I_n^{(s)} = -i\int_\Gamma f^{(s)}(a, b) g_0(0, b) e^{(n-1)ika}\, d\Gamma,$$

$$I_n^{(g)} = -i\int_\Gamma f_j^{(g)}(a, b) g_0(0, b) e^{(n-1)ika}\, d\Gamma.$$

Note that R, T are the reflection and transmission coefficients, β_R, β_T are the associated phase shifts, $^{(s)}, ^{(g)}$ denote components associated with the scattered and generated potentials respectively and j denotes components associated with the jth mode of motion of the body.

BOUNDARY ELEMENT DISTRIBUTION

In practice, the number of elements into which the source distribution boundary is subdivided is limited by available computer storage space. Apart from this physical limitation, the fact that the run-time for any particular solution is roughly proportional to the square of the number of elements emphasizes the importance of restricting the number of elements to the minimum required for an acceptably accurate solution.

To ensure an adequate representation of the object boundary subject to the above limitations, Hogben *et al.*[7] have recommended the following guidelines, based on experience, for fixed three-dimensional objects:

1. Elements should be concentrated in areas where the body geometry (slope or curvature) changes rapidly with position.
2. Individual element dimensions should not exceed the local radius of curvature.
3. No element dimension should exceed 1/8 of the incident wavelength.
4. Element dimensions should change gradually between areas of high and low concentrations.
5. The dimensions of an element should not be more than 50% greater than those of neighbouring elements. If several small elements surround a larger one, the accuracy is that associated with the large element, resulting in an inefficient distribution.

In the case of two-dimensional floating bodies, the author is unaware of the availability of similar guidelines. However, it may be reasonably assumed that the principles remain the same.

In the case of an immersed surface which is substantially rectangular, the following formulation has been adopted to comply with the above recommendations. Element parameters (see Figure 2) may be defined thus:

maximum element length on a vertical side $= a_{\max}$,
maximum element length on the base $= b_{\max}$,
number of elements on the straight portion of each side $= N_s$,
number of elements on the straight portion of the base $= 2N_b + 1$,
number of constant length elements on each radial edge $= N_c$,
minimum element size $= \gamma_{\min}$,
submerged edge radius $= R$.

If it is assumed that the minimum element length occurs on the radial edges, it may be stated that

minimum element length $\gamma_{\min} = \pi R/2N_c$

The element distribution may be defined thus:

side elements

$$\gamma_1^{(s)} = a_{\max},$$
$$\gamma_i^{(s)} = a_{\max}\alpha^{i-1}, \quad i = 1, 2, \ldots, N_s, \quad \alpha \leqslant 1;$$

base elements

$$\gamma_1^{(b)} = b_{\max}$$
$$\gamma_j^{(b)} = b_{\max}\beta^{j-1}, \quad j = 1, 2, \ldots, N_b, \quad \beta \leqslant 1;$$

constant length radial edge elements

$$\gamma_c = \pi R/2N_c,$$

where subscript i denotes the ith vertical element from the free surface, α denotes the constant element length ratio pertaining to each vertical side, subscript j denotes the jth horizontal element from the centroidal axis, β denotes the constant element length ratio pertaining to the base and subscript c denotes a constant length element on a submerged radial edge.

Starting from a specified minimum element length dependent on the number of constant length elements on the submerged radial edges, and a nominal element length ratio, the precise element

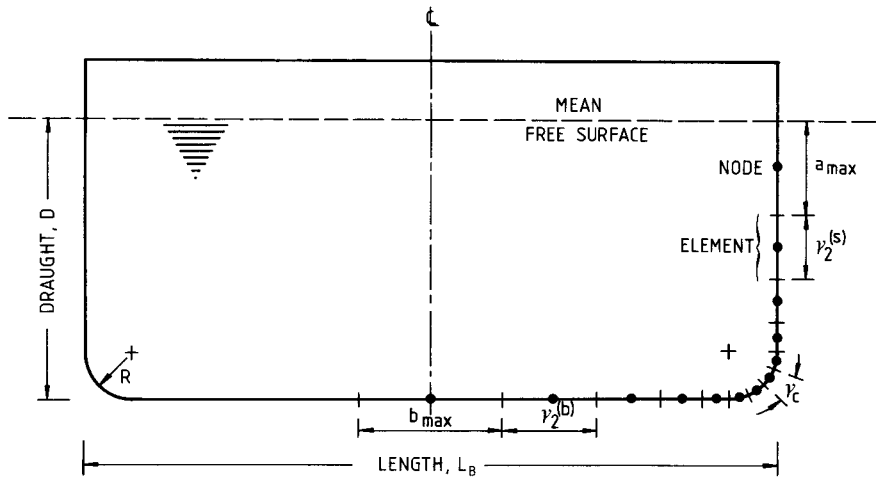

Figure 2. Definitions for boundary element distribution

length ratio is computed from an iterative procedure. If the same nominal element length ratio is used for both side and base elements, this results in a roughly symmetric increase in side and base elements away from the submerged radial edge of the body. Depending on the aspect ratio of the immersed surface, the computed element length ratios generally differ by only a few per cent either side of the nominal input value.

RESULTS AND DISCUSSION

Based on the foregoing analysis, solutions have been evaluated for three substantially rectangular obstacles with immersed profile aspect ratios of 2, 4 and 8 respectively, full details of which are given in the Appendix.

The far-field reflection and transmission coefficients, for both 'fixed' and 'floating' mode, have been evaluated from equations (28). The motion response of the body, suitably non-dimensionalized with respect to the incident wave amplitude, has been evaluated from equation (27). In order to investigate the sensitivity of solutions to changes in numerical discretization of the immersed profile of the obstacle, the evaluations have been carried out for a range of values of the element length ratio (ELR) in conjunction with a specified number (N_c) of constant length radial edge elements and *vice versa*. Element distribution details for each obstacle are given in the Appendix. Since the hydrodynamic interaction parameters depend essentially on the relative size of obstacle and incident wave, solutions have been evaluated over a suitable range of values of the non-dimensional diffraction parameter L_B/L.

For reasons of brevity, graphical presentation of results has been limited to those pertaining to obstacle number 2 (see Appendix) with an immersed profile aspect ratio of 4. These can be seen in Figures 3–8.

Fixed mode

In general for the three obstacle configurations investigated, the fixed mode reflection and transmission coefficients exhibit very little sensitivity to changes in discretization level throughout the whole range of diffraction parameter values. Notwithstanding a slight increase in

discretization-related sensitivity with decreasing obstacle draught, the solution variation resulting from a substantially increased level of discretization (see Tables II and III) can be regarded as insignificant for all practical purposes. It would thus appear that the three-dimensional discretization recommendations of Hogben *et al.*[7] apply equally to two-dimensional fixed obstacles.

As first pointed out by John,[8] the integral equation develops eigenfunctions for surface-piercing obstacles at certain values of the diffraction parameter L_B/L. At these 'irregular' frequencies, each eigensolution represents a non-trivial source distribution which leaves the external flow field undisturbed and is a numerical rather than a hydrodynamic feature resulting from coincidence of

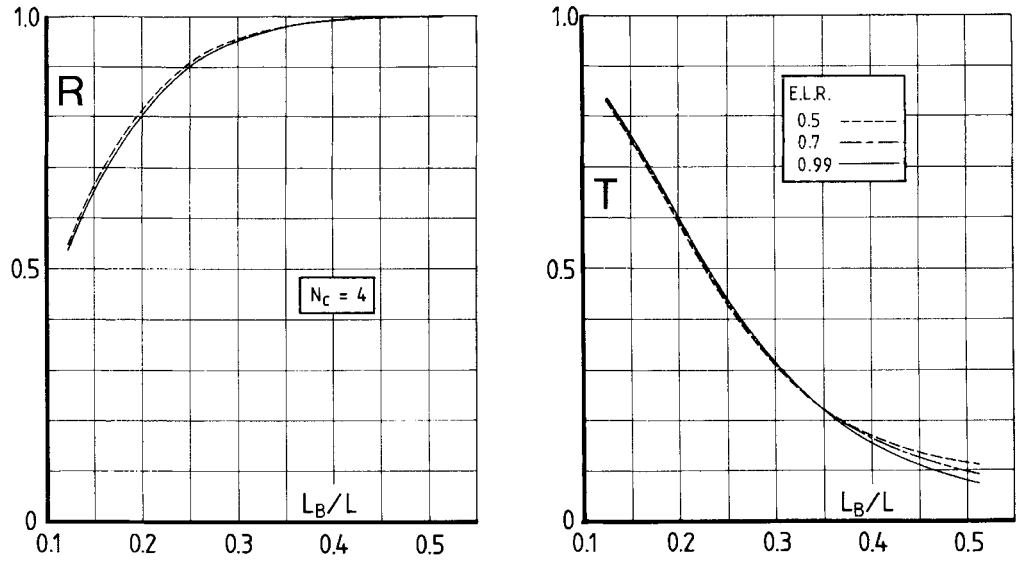

Figure 3. Fixed obstacle reflection and transmission ($N_c = 4$; ELR variable)

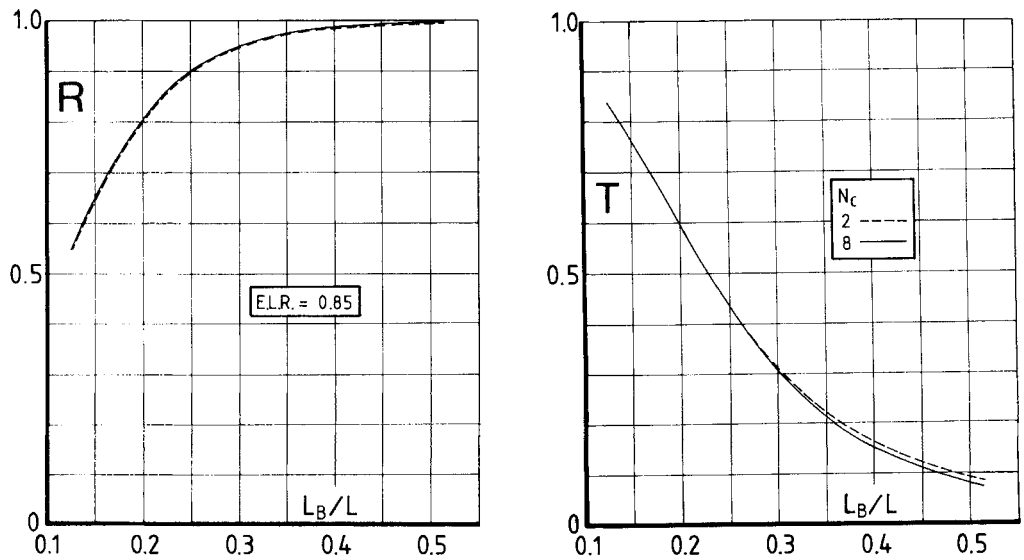

Figure 4. Fixed obstacle reflection and transmission (ELR = 0·85; N_c variable)

source and obstacle boundaries. Examination of the results for all three obstacles indicates that the divergence of transmission coefficients with increasing diffraction (Figures 3 and 4) is attributable to the proximity of the first irregular frequency and is not diffraction-related. The results show clearly that the effect of such numerical instability can be reduced by increasing the level of immersed profile discretization as first indicated by Frank.[9]

Floating mode

The results presented in Figures 5 and 6 demonstrate clearly that, notwithstanding the difference in overall behavioural trends, the floating mode reflection and transmission coefficients are

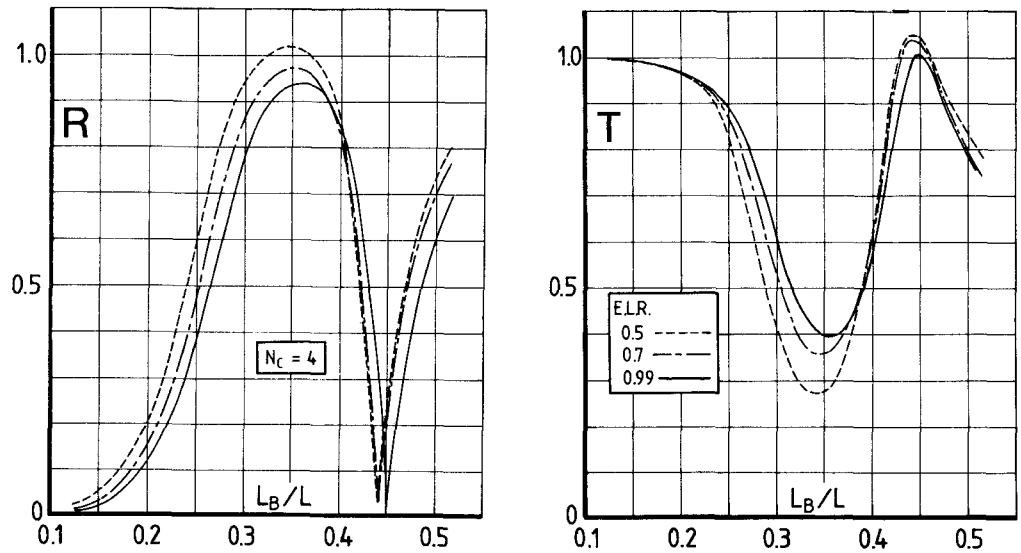

Figure 5. Floating obstacle reflection and transmission ($N_c = 4$; ELR variable)

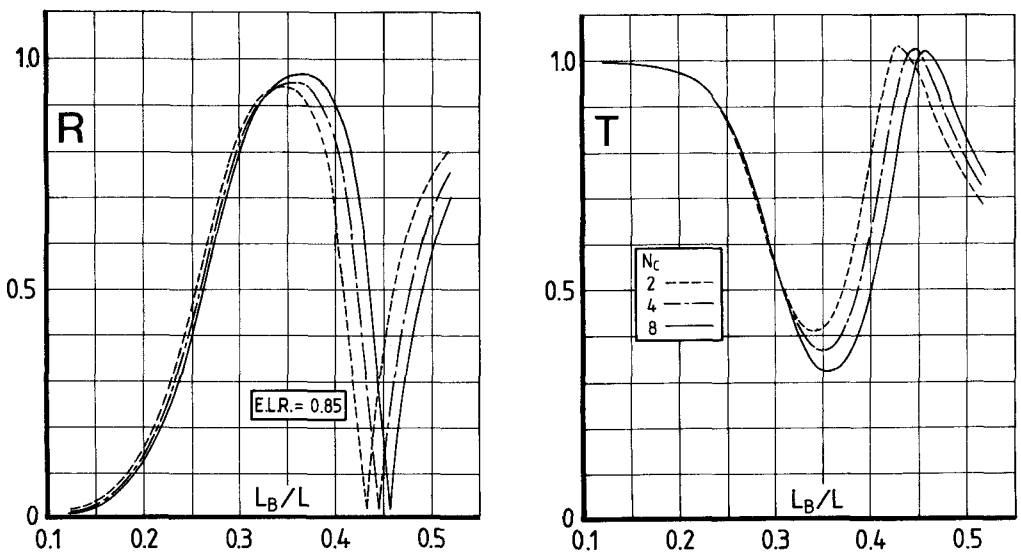

Figure 6. Floating obstacle reflection and transmission (ELR = 0·85; N_c variable)

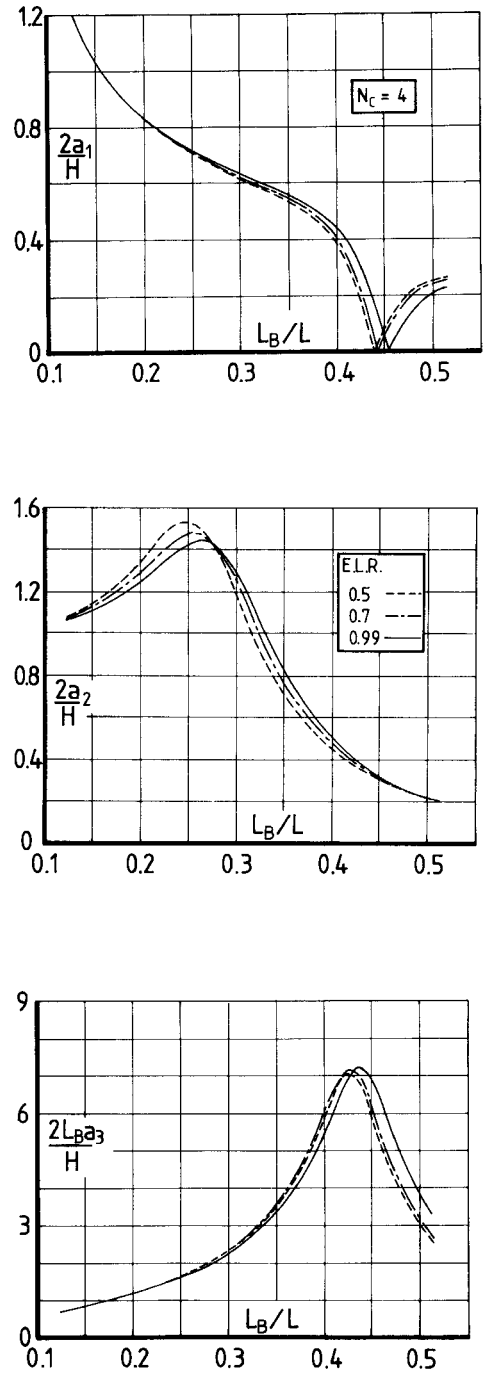

Figure 7. Floating obstacle motion response ($N_c = 4$; ELR variable)

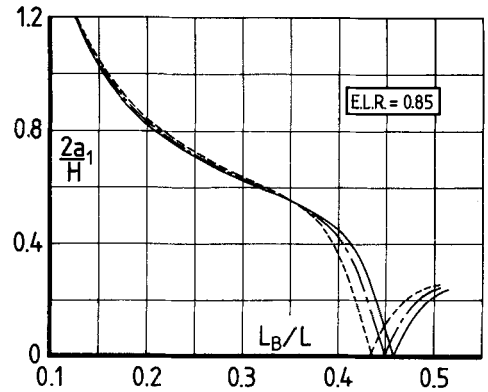

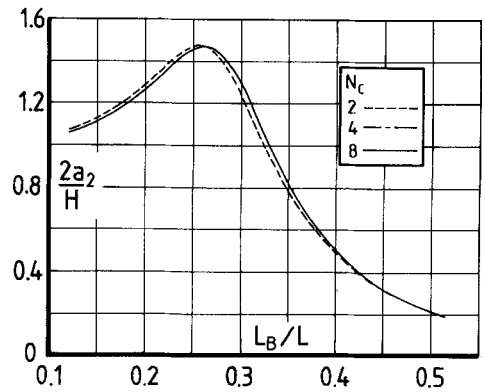

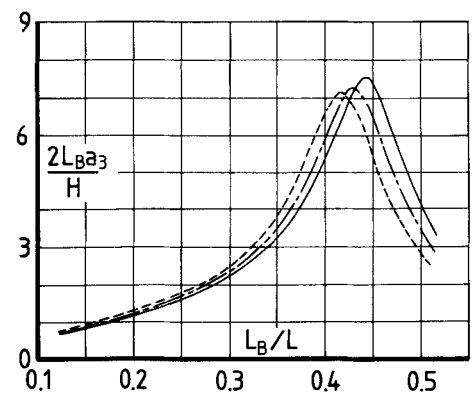

Figure 8. Floating obstacle motion response (ELR = 0·85; N_c variable)

significantly more sensitive to changes in discretization level than the equivalent fixed mode results. Since the discretized solution of the integral equation entails the use of a common coefficient matrix, it must be concluded that the increased sensitivity is attributable to the three additional degrees of freedom associated with the floating mode. The general trend of floating obstacle solutions in Figures 5–8 indicates that, unless the level of immersed surface discretization is considerably increased from that employed in this study, the errors which may be associated with each solution are greater than would be acceptable for practical purposes. Apart from the possible introduction of numerical instability due to matrix ill-conditioning, the substantially increased computer memory and time requirements resulting from such an increase in discretization level would render use of this method largely impracticable. In order to obtain solutions which are accurate within acceptable tolerance limits while maintaining computer requirements at a practicable level, the use of higher-order (linear and quadratic) elemental source strength distributions is therefore suggested for the analysis of floating obstacle hydrodynamics.

Figures 7 and 8 illustrate two interesting trends which pertain to the motions of all three obstacle configurations investigated: the discretization-related sensitivity of the interrelated surge and pitch solutions increases consistently with increasing wave diffraction, while heave solution sensitivity increases within frequency domains adjacent to the obstacle resonant frequency; heave solutions are consistently more sensitive to changes in element length ratio than to changes in radial edge element density, while the converse is true for surge and pitch solutions. This would suggest that, for a given value of the diffraction parameter, the level of immersed profile discretization required to produce solutions of equivalent accuracy is different for each mode of motion, thus providing further indication of the need for higher-order source strength distributions.

CONCLUSIONS

1. The Green function integral equation method, assuming constant elemental source strength, gives solutions within acceptable tolerance limits for fixed obstacle hydrodynamics in a two-dimensional domain.
2. For the case of substantially rectangular fixed obstacles, a considerable saving in computational time and memory requirements may be effected by the use of a non-uniform distribution of elements over the immersed profile of the obstacle, subject to the recommendations contained herein.
3. For substantially rectangular floating obstacles, the assumption of constant elemental source strength results in insufficiently accurate solutions at practicable levels of immersed surface discretization, indicating the need for higher-order (linear and quadratic) elemental source strength distributions.

ACKNOWLEDGEMENTS

The study reported herein was carried out in the Civil Engineering Department of The City University, London, and was made possible by the award of maintenance and support grants by The Science and Engineering Research Council.

APPENDIX. OBSTACLE DETAILS AND ELEMENT DISTRIBUTION DATA

Obstacle details

The numerical study presented in this paper was carried out in conjunction with an experimental investigation of the behaviour of floating obstacles in regular waves.[10] Owing to the nature of the

experimental apparatus, the horizontally acting mass and stiffness parameters in equation (27) include additional components of mass and spring restraint stiffness respectively. Full details are given in Table I.

Table I. Obstacle geometric and inertial details

Body number	1	2	3
Length (m)	0·96	0·96	0·96
Draught (m)	0·48	0·24	0·12
Immersed surface aspect ratio	2	4	8
Immersed edge radius (m)	0·12	0·06	0·03
Centroidal y co-ordinate (m)	−0·283	−0·118	0·034
Metacentric height (m)	0·208	0·317	0·552
Horizontally acting mass/m width (kg)	497·9	270·8	153·7
Vertically acting mass/m width (kg)	458·5	231·4	114·3
Moment of intertia/m width (kg m^2)	26·59	14·14	10·80
Horizontal spring restraint/m width (N m^{-1})	371·9	278·9	185·9
Still water depth (m)	1·2	1·2	1.2

Element distribution data

Table II. Number of immersed surface elements ($N_c = 4$ throughout)

Body number	Element length ratio		
	0·50	0·70	0·99
1	17	21	37
2	19	25	55
3	21	29	87

Table III. Number of immersed surface elements (ELR = 0·85 throughout)

Body number	number of elements per radial edge		
	2	4	8
1	15	27	45
2	21	33	53
3	27	41	62

REFERENCES

1. C. J. Garrison, 'Hydrodynamic loading of large offshore structures—three-dimensional source distribution methods', in O. C. Zienkiewicz, R. W. Lewis and K. G. Stag (eds), *Numerical Methods in Offshore Engineering*, Wiley, Chichester, 1978, pp. 87–140.
2. J. V. Wehausen and E. V. Laitone, 'Surface waves', *Handbuch der Physik*, **9**, Springer, Berlin, 1960, pp. 446–778.
3. R. A. Naftzger and S. K. Chakrabarti, 'Scattering of waves by two-dimensional circular obstacles in finite water depths', *J. Ship Res.*, **23**, 32–42 (1979).
4. T. Sarpkaya and M. de St. Q. Isaacson, *The Mechanics of Wave Forces on Offshore Structures*, Van Nostrand Reinhold, New York, 1981, ch. 6.

5. J. V. Wehausen, 'The motion of floating bodies', *Ann. Rev. Fluid Mech.*, **3**, 237–268 (1971).
6. J. N. Newman, 'The exciting forces on a moving body in waves', *J. Ship Res.*, **9**, 190 (1965).
7. N. Hogben, J. Osborne and R. G. Standing, 'Wave loading on offshore structures: theory and experiment', *Proc. Symp. on Ocean Engineering*, National Physical Laboratory, London, RINA, 1974.
8. F. John, 'On the motion of floating bodies II', *Comm. Pure Appl. Math.*, **3**, 45 (1950).
9. W. Frank, 'Oscillations of cylinders in or below the free-surface of deep fluids', *NSRDC Report No. 2375*, Washington D.C., 1967.
10. K. J. Williams, 'The dynamics of floating bodies in a regular wave environment', *Ph.D. Thesis*, The City University, London, 1986.